

## Nano-Structures and Interactions of Alkali Metals within Silica Gel

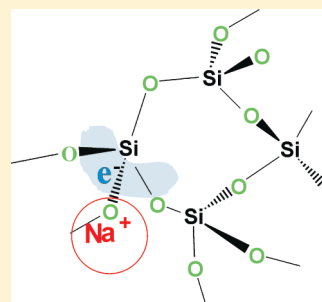
James L. Dye,<sup>\*,†</sup> Partha Nandi, James E. Jackson, Michael Lefenfeld,<sup>\*,‡</sup> Philip A. Bentley, Bryan M. Dunyak, Frank E. Kwarcinski, Christopher M. Spencer, Thomas N. Lindman, Peter Lambert, Peter K. Jacobson, and Mikhail Y. Redko

<sup>†</sup>Department of Chemistry, Michigan State University, East Lansing, Michigan 48824, United States

<sup>‡</sup>SiGNa Chemistry, Inc., 530 E. 76th Street, Suite 9E, New York, New York 10021, United States

## Supporting Information

**ABSTRACT:** Liquid alkali metals and their alloys can be absorbed into the 15 nm diameter pores of nanostructured silica gel (SG) at loadings up to 40 wt %. Characterization of the resultant materials was done by measuring the amount of hydrogen produced by addition of alcohols and/or water, by differential scanning calorimetry, and by static  $^{23}\text{Na}$  NMR spectroscopy. While sodium must be heated above 100 °C to form Na in SG, absorption of Na–K alloys at ambient temperatures yields nanoscale metallic clusters in the pores (Stage 0). In both cases, some of the encapsulated metal may dissolve in the silica and ionize to produce highly mobile  $\text{M}^+$  ions with reversible electron transfer to the silica. This presumption is consistent with literature observations that sodium is soluble in silica films at ambient temperatures at levels up to 35 mol percent and is presumed to form highly mobile  $\text{Na}^+\text{O}^-$  species (Lagarde, P.; Flank, A.-M.; Mazzara, C.; Jupille, J. *Surf. Sci.* **2001**, 482–485, 376–380). Heating M-SG materials leads to reduction of  $\text{SiO}_2$  to form material that contains localized  $\text{M}^+\text{O}^-$  species and Si–Si bonds in increased proportion as the temperature and time of heating are increased. Above 350 °C, elemental silicon, alkali metal silicides, and alkali metal silicates are formed. The dissolution and reaction of potassium from encapsulated Na–K alloys occurs preferentially over that of sodium. Irreversible reaction even occurs at room temperature over a period of months. The temperature dependence of solid state  $^{23}\text{Na}$  NMR spectra indicates the presence of rapid exchange between  $\text{Na}^0$  in the metal clusters and  $\text{Na}^+$  at the walls (and perhaps within the silica).



**KEYWORDS:** alkali metals, sodium, silica–gel,  $^{23}\text{Na}$  NMR, silicates, silicides

## INTRODUCTION

The ability to encapsulate up to 40 wt % alkali metals in the nanoscale pores of silica gel (SG) has led to convenient, powerful reducing agents for organic synthesis.<sup>1,2</sup> Heating these materials leads to conversion from metallic clusters in the pores (Stage 0) with the likelihood of some reversible solubility in the silica, to chemical reaction with the silica framework. It is the object of the present work to describe the nature of these changes and their effects on the properties of metal-silica gel (M-SG) powders.

The reaction between alkali metals and silica at elevated temperatures has been known for many years.<sup>3–5</sup> Anyone who has heated sodium in glass or fused silica has seen the brown coloration that occurs, although the detailed nature of the species responsible is still uncertain. In efforts to take advantage of the powerful reducing properties of alkali metals, many inert supports for alkali metals have been used,<sup>6</sup> including graphite,<sup>7</sup> colloidal silica,<sup>8</sup> alumina,<sup>9</sup> other metal oxides,<sup>10</sup> and even sodium chloride.<sup>11</sup> The main objective of these studies was the preparation of solid reducing materials that could avoid the need to use either alkali metal dispersions in a hydrocarbon or solutions in liquid ammonia.

Alkali metals have been introduced from the vapor phase into *alumino-silicate* zeolites since the 1960s.<sup>12,13</sup> Ionization occurs to yield electrons trapped by clusters that include pre-existing cations.<sup>14</sup> When alkali metals are introduced from the vapor phase into the pores of *pure silica* zeolites, the resulting metallic clusters or chains

undergo at least partial ionization to form cations trapped at the walls and, according to theory,<sup>15</sup> electrons in the open spaces.<sup>16–18</sup> Metal-loaded zeolite powders retain the reducing ability of the parent metals and can be loaded with up to about 12 mol percent alkali metal (based on  $\text{SiO}_2$ ).

We subsequently found that *liquid* alkali metals and their liquid alloys could be absorbed into the pores of nanostructured silica (silica gel, SG) at loadings up to 40 wt % (59 mol % for Na) and that suitable heat treatment yielded samples that contained both alkali metal nanoparticles and alkali cations.<sup>1,2</sup> Of major importance to their use as reducing agents, alkali metal-silica gel (M-SG) materials are nonstatic, free-flowing powders that are stable and can be weighed to provide known amounts of reducing equivalents. Samples can be prepared as nonpyrophoric powders that are stable in *dry* air. As a result, they are useful in organic synthesis<sup>19–23</sup> and are commercially available for this purpose.<sup>24</sup> Since they can still react with moisture, which decreases reducing equivalents, they should be handled with care, but their free-flowing character, long-term stability, and inert, nontoxic products make them attractive replacements for other powerful reducing agents.

Studies by others have shown that sodium metal, deposited on thin, amorphous silica films at 300 K, is soluble to levels as high as

**Received:** January 17, 2011

**Revised:** March 24, 2011

**Published:** April 12, 2011

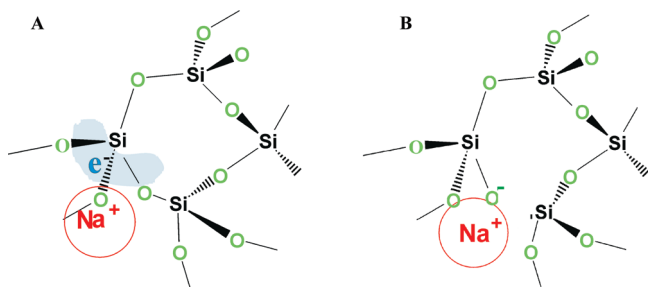


**Figure 1.** Alternative models of reversible ionization of sodium dissolved in silica films. (A) Coordination of Na<sup>+</sup> to three oxygens by electron transfer to delocalized excited state orbitals without Si–O bond breakage. (B) Si–O bond breakage and formation of a Na<sup>+</sup>–O<sup>−</sup> ionic bond. The radical formed according to this model would be very likely to react with additional Na<sup>0</sup> to form Na<sup>+</sup> and an anion.

35 mol percent (20 wt %) and that it is present as Na<sup>+</sup>.<sup>25,26</sup> Reversible incorporation and diffusion of sodium in such non-porous films at ambient temperatures show that the dissolved sodium is mobile. Models of the mobility mechanism suggest localization times as short as a few picoseconds.<sup>27</sup> Thus, any reaction between the mobile Na and SiO<sub>2</sub> at ambient temperatures, such as Si–O–Si reaction with Na to produce Na<sup>+</sup>–O<sup>−</sup>–Si moieties, must be fast and reversible. It is clear from extended X-ray absorption fine structure (EXAFS) and X-ray photoelectron spectroscopy (XPS) studies<sup>25–27</sup> of such films at 300 K that Na<sup>0</sup> is converted to Na<sup>+</sup>, which is coordinated to three oxygens, and that there is little reorganization of the silica structure. The Na<sup>+</sup>–O and Na<sup>+</sup>–Si distances are close to those in soda-silica glasses, and the oxygen-1s XPS data are similar to those associated with O<sup>−</sup> bound to only one silicon (“non-bridging oxygen”). These results and molecular simulations<sup>28</sup> suggested that the electron released by ionization of Na<sup>0</sup> is transferred to oxygen with breakage of an adjacent Si–O bond. But, according to the EXAFS data<sup>27</sup> the three oxygens coordinated to Na<sup>+</sup> are equivalent, so the processes must be very rapid and reversible. A suggested alternative to breakage of the Si–O bond is transfer of the electron to empty orbitals that involve both silicon and oxygen.<sup>27</sup> This could yield high mobility of Na<sup>+</sup> and e<sup>−</sup> without the need to break and remake Si–O bonds. Two possible models are diagrammed in Figure 1. Another feature that is characteristic of dissolved Na in SiO<sub>2</sub> films at ambient temperatures is the prevalence of dimers of sodium ions at concentrations above 10 mol percent.<sup>25</sup> The Na–Na distance (0.29 nm) is shorter than that in sodium metal (0.37 nm) and suggests the close approach of two oxygen-coordinated Na<sup>+</sup> ions and their associated electrons.

The nonporous silica films described above were prepared by oxidation of silicon and were studied under ultrahigh vacuum. Thus, while they are very different from the nanoporous silica gel used in our studies, the possibility of low-temperature reversible transfer of alkali metals from the silica gel pores to the silica framework must be considered.

Our previous work provided an overview of the species present when alkali metals enter the pores of silica gel at low to moderate temperatures.<sup>1,2,18</sup> Species identification included pair-distribution function (PDF) studies by X-ray scattering and solid state <sup>23</sup>Na NMR measurements.<sup>2</sup> Liquid Na–K alloys fill the pores with metal at room temperature to form Stage 0 material (M-SG-0). No Na<sup>+</sup> is formed at this stage, except for the 1–2% formed by reaction of the metal with residual SiOH groups. Upon heating M-SG samples to 120–150 °C for 12–24 h, conversion

to a second form (originally designated as Stage I) occurs. PDF studies showed the presence of nanocrystalline metal particles, while <sup>23</sup>Na NMR measurements showed that both Na<sup>0</sup> and Na<sup>+</sup> are present in such samples.<sup>2</sup> The variation of the Na<sup>0</sup>/Na<sup>+</sup> ratio at various metal concentrations and silica gel pore sizes led us to conclude that the fraction of metal ionized depends on the relative number of available sites for Na<sup>+</sup>. At low metal concentrations or with smaller pore sizes, a larger fraction of the metal is ionized, presumably because of thermodynamically favored complexation of M<sup>+</sup> at surface or internal sites of silica. A remaining puzzle was the fate of the released electrons. Our initial speculation was that they formed a mobile electron layer near the surface, similar to that proposed for silica zeolites.<sup>17</sup> However, the concentration of Na<sup>+</sup> at saturation is generally greater than can be accommodated only at surface sites. According to the thin film work referred to above, reversible solubilization of sodium in the silica framework may occur, accompanied by ionization. A major question addressed in this work is the conversion of such mobile dissolved alkali metals to localized M<sup>+</sup>–O<sup>−</sup>–Si and Si–Si moieties as functions of time and temperature.

In spite of their simple composition (M + SiO<sub>2</sub>) metal-silica gel materials are complex and unlike any other materials. Mild heating results in irreversible reaction of a fraction of the metal, and higher temperatures yield still more complex materials as the silica is reduced, ultimately forming metal silicates, silicon, and metal silicides. Although we can only infer the nature of some of the processes and species formed, the experiments described here provide new insights into the interaction of alkali metals in the pores of silica gel with the silica framework that surrounds the pores.

## EXPERIMENTAL SECTION

Silica gel samples with nominal pore diameters of 15, 6, and 3 nm and alumina gel with 9 nm pores were obtained from W. R. Grace, Inc. and were calcined in air at 600 °C for 24 h to remove water and decrease the reducible surface OH content. The synthesis and heat treatment of M-SG samples, as well as the instrumentation for NMR, PDF, magnetic susceptibility, and <sup>23</sup>Na NMR studies have been previously described.<sup>2</sup> Alkali metals and Na–K alloys were prepared and added to silica gel in a helium-filled glovebox, and all samples removed from the box were in sealed containers to avoid exposure to air and moisture. Appropriate heat-treatment produced samples that were nonpyrophoric and could be handled briefly in air. The Differential Scanning Calorimetry (DSC) studies utilized a Thermal Analysis Q-200 instrument. Solid-state <sup>23</sup>Na NMR spectra were obtained with samples sealed under vacuum in 5 mm diameter fused silica tubes. Powder X-ray diffraction (PXRD) utilized a Rigaku Rotaflex RU-200 B diffractometer while Raman spectra were measured with a Specs 1250 –1.25 m spectrometer.

The reducing capacity of all M-SG samples (expressed as the weight percent metal equivalent) was measured by a hydrogen collection process. The amount of hydrogen collected in each step was determined by measuring the pressure and volume, with appropriate correction for solvent vapor pressures. The pressure was measured with a CeComp 0–760 Torr digital pressure gauge. All M-SG samples produce hydrogen quantitatively upon addition of water (except for the small loss due to reaction with residual SiOH groups during preparation). Samples that have been heated to 300 °C or above (called Stage II) do not react appreciably with simple alcohols (methanol, ethanol, iso-propanol). Subsequent addition of water yields quantitative total hydrogen production.

## RESULTS AND DISCUSSION

**Overview of Processes.** Previous studies by us and others, and the overall results of this work, provide a general picture of

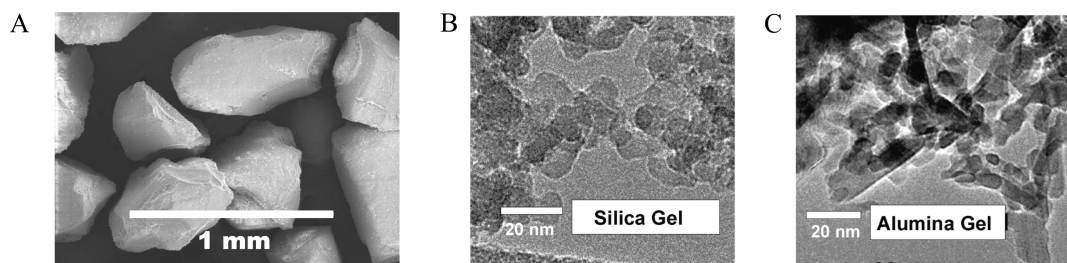


**Figure 2.** Electron micrographs of the materials used in this work. (A) Silica gel particles of diameter 0.3–0.5 mm. (B) Transmission electron microscopy (TEM) image of amorphous silica gel with 15 nm nominal pore diameters. (C) TEM image of alumina gel with 9 nm pore diameters. Nanocrystals of  $\gamma$ -alumina are evident.

the nature of M-SG materials. Inclusion of Na–K alloys in the nanoscale pores by direct combination of the liquid alloy and silica gel occurs, possibly with reversible solubilization of part of the metal in the silica, but without significant heat production. This is referred to as Stage 0 material. Density measurements show that no appreciable expansion occurs, so the maximum amount of metal that can be included is determined by the pore volume. The silica framework may interact with the alkali metal in several ways. The simplest way (but for which we have no direct evidence) is solution of the metal in the amorphous silica and its ionization to form mobile  $M^+$  and  $e^-$ , with either rapid reversible breakage of Si–O bonds and formation of  $M^+-O^--Si$  units or coordination of  $M^+$  to three oxygens of a silica tetrahedron with electron transfer to unoccupied excited states of the silica. If the latter occurs, increased temperature causes irreversible Si–O bond breakage and  $M^+$  localization (Stage I). As the amount of dissolved metal increases, closely spaced pairs of  $M^+$  ions form, leading to Si–Si bond formation in addition to  $M^+-O^--Si$  species (Stage II). These processes are greatly accelerated by heating, and both occur to extents that depend on the temperature and time of heating. Since sodium melts at 97.8 °C, the addition of liquid sodium to silica gel cannot form pure Stage 0 Na-SG; some Stage I and Stage II material is always present. Reaction of alkali metals with silica ultimately yields metal silicates, metal silicides, and elemental silicon at temperatures above 350 °C. Prior to phase separation of these end products, apparently homogeneous Stage II material forms as a continuous network of Si–O and Si–Si bonded material. Annealing a sample of Na-SG at 400 °C for several days yields crystalline silicon. This was verified by the appearance of the Raman peak of crystalline silicon at 518.7  $cm^{-1}$  (Supporting Information, Figure 1S). Since silicon reacts with sodium at this temperature, the presence of excess sodium also produces sodium silicide, as demonstrated by PDF studies and solid state  $^{23}Na$  NMR.<sup>2</sup>

**Preparation.** Most of the studies described here utilized silica gel with nominal pore diameters of 15 nm and a surface area of 300  $m^2 g^{-1}$ , although some experiments used SG with 6 and 3 nm nominal pore diameters. Each SG granule (Figure 2A) contains interconnected amorphous  $SiO_2$  nanoparticles with diameters comparable to those of the interparticle pores (Figure 2B). Alumina gel (AG) with 9 nm nominal pore diameters consists of interconnected nanocrystals of  $\gamma$ -alumina (Figure 2C). Both SG and AG are useful carriers for alkali metals because they are resistant to chemical reduction at low and moderate temperatures. As obtained, they contain some water and surface SiOH or AlOH groups that would react with alkali metals to produce hydrogen. Calcination in air at 600 °C eliminates all but a few percent of these reactive groups. A direct measurement of the amount of residual SiOH groups (1.7 mol

percent) in one sample was obtained by measuring the hydrogen produced when liquid  $Na_2K$  alloy was added to calcined SG.

Stage 0 M-SG can be made at ambient temperatures by interaction of a liquid alkali metal or alloy with silica gel. We have prepared samples that range from  $K_5Na$ -SG to  $Na_3K$ -SG in this way. Most of our studies of Stage 0 M-SG used either  $K_2Na$  or  $Na_2K$  combined with calcined silica gel. The products are shiny, black, pyrophoric powders. Solid state  $^{23}Na$  NMR studies of  $Na_2K$ -SG-0 show only peaks of metallic sodium plus a small peak of  $Na^+$  from the product of reaction with residual Si–OH groups.

**Differential Scanning Calorimetry.** DSC traces of eight fresh samples of  $Na_2K$ -SG-0 and three of  $K_2Na$ -SG-0 show melting endotherms of the encapsulated metal, with  $\Delta H_{melt}$  (compared with the bulk metal) reduced to  $35 \pm 6\%$  and  $53 \pm 7\%$  percent, respectively. The corresponding average value for 20 samples of Na-SG is  $39 \pm 7\%$ . These decreases in the heat of melting could result from decreases in the percent present as metal, distributions into small sites, and/or the effect of particle size on the enthalpy of melting. For example, the heat of melting of indium metal in controlled-pore glasses with 18 nm diameter pores is only half that of bulk indium.<sup>29</sup>

There is an important indicator that not all of the reduction in  $\Delta H_{melt}$  is due to the small size of the metal inclusions. This is provided by DSC studies of Na and  $Na_2K$  in alumina gel (AG). In contrast to SG, alkali metals do not dissolve in the AG framework or react with it at the temperature of preparation. Even though the average pore diameter is smaller (9 nm) than that of the SG used (15 nm), the melting endotherms of many M-AG samples are only reduced to 70–90% of the bulk metal value, rather than the greater reduction seen for M-SG samples. This could be the result of reversible solubility in SG, although we have no direct evidence of this. Thus, while changes in the melting endotherm upon heating can be used as a measure of the decrease in encapsulated metal content, the fraction of metal present in the pores cannot be determined solely from the reduction in the enthalpy of melting compared with that of the bulk metal.

The small size of the alkali metal inclusions also resulted in a decrease in the melting temperature, a common occurrence.<sup>29,30</sup> Bulk  $K_2Na$  and  $Na_2K$  alloys melt sharply at  $-12.6$  and  $+6.9$  °C, respectively. 40 wt % Stage 0 samples in SG gave broad melting endotherms starting at  $-39$  and  $-13$  °C and peaking at  $-28$  and  $-5$  °C, respectively. The melting temperature of sodium nanoparticles in Na-SG is  $66 \pm 2$  °C, some 32 °C below the bulk melting temperature.

We do not have direct measures in this work of the amount of reversible solubilization of alkali metals in SG at room temperature nor the time required to reach saturation. However, the solid-state  $^{23}Na$  NMR measurements to be considered later



provide clear evidence for  $\text{Na}^0\text{--Na}^+$  exchange on the micro-second time scale. While this could involve only exchange with the estimated 5–9%  $\text{Na}^+$  level on the surface, exchange of  $\text{Na}^0$  with  $\text{Na}^+$  dissolved in silica cannot be ruled out. Thin film studies indicate that sodium metal dissolves reversibly in amorphous silica at ambient temperatures, ionizes, and is highly mobile.<sup>25–27</sup>

Although liquid alkali metals enter the pores of silica gel as metallic nanoparticles, and presumably dissolve to some extent in the silica, they undergo a series of complex reactions upon heating (as described in the next section). The processes that occur upon heating, dissolution of the metal in the silica framework,  $\text{M}^+$  localization at  $\text{Si--O}^-$  sites, and the formation of  $\text{Si--Si}$  bonds, all cause ionization to give  $\text{M}^+$ , but the extent of the heat release due to each process cannot be directly determined. The preparation of Stage 0 Na–K alloys in silica gel at room temperature occurs without the production of appreciable heat. From the maximum temperature increase during preparation, the estimated maximum value of  $\Delta H$  is only  $-2$  kJ per mole of metal. Thus, the formation of Stage 0 samples, in which the metal moves from the bulk into the pores and may partially dissolve in the silica, is nearly thermo-neutral. The overall exothermic enthalpy change,  $\Delta H_{\text{exo}}$ , obtained with DSC scans from 50 to 450 °C, results from the reduction of  $\text{SiO}_2$  to form  $\text{Si--Si}$  and  $\text{M}^+\text{--O}^-\text{Si}$  bonds, and, ultimately, from complete reaction to form a mixture of silicates, silicon, and metal silicides. Thus, differences in the value of  $\Delta H_{\text{exo}}$  per mole of metal (kJ/mol M) with time and/or heat treatment provide a direct measure of the enthalpy change for the processes involved. Similarly, changes in  $\Delta H_{\text{melt}}$  can be used to determine the fraction of metal remaining in the pores after treatment, compared with that initially present.

Eight samples of freshly prepared 40%  $\text{Na}_2\text{K-SG-0}$  yielded an average molar  $\Delta H_{\text{exo}}$  of  $-63 \pm 7$  kJ/mol M while three samples of  $\text{K}_2\text{Na-SG-0}$  gave  $-71 \pm 5$  kJ/mol M. The formation of Na-SG requires elevated temperatures and long reaction times, so both solubilization of sodium in the silica and its reaction to form localized  $\text{Na}^+$  always occurs to some extent during preparation. The average value of the molar  $\Delta H_{\text{exo}}$  for 21 samples of Na-SG was  $-34 \pm 8$  kJ/mol M.

The kinetics of heat evolution is complicated by the heterogeneous nature of the samples. To react with the silica, alkali metal must first move from the pores into the silica framework. Although film studies (with thicknesses comparable to the silica particle diameters in SG) showed that sodium is reversibly soluble in amorphous silica films at 300 K, there are no data on the rate of this process nor whether it involves heat production.<sup>25</sup> Unlike thin amorphous silica films, the silica gel used in this work contains nanoscale pores of various sizes that can encapsulate sodium. The complex internal surface regions may provide preferential sites for ionization of sodium as well as for trapping small sodium clusters.

Since fresh samples of  $\text{Na}_2\text{K-SG-0}$  contain alloy in the pores that has not yet reacted irreversibly with the silica, they provide the opportunity to study the temperature–time behavior of the exothermic reaction of alkali metals with silica. Changes in the amount of alkali metal remaining in the pores can be monitored by measuring the enthalpy of melting. A sample of  $\text{Na}_2\text{K-SG-0}$  stored at  $-30$  °C for three months showed no significant change in the DSC pattern, while storage at ambient temperatures caused a marked decrease in the magnitude of the  $-5$  °C endotherm, accompanied by the build-up of an endotherm at  $\sim +5$  °C that shifted to 20 °C after 22 days and to 28 °C after 142 days. The same general behavior was seen for two other samples

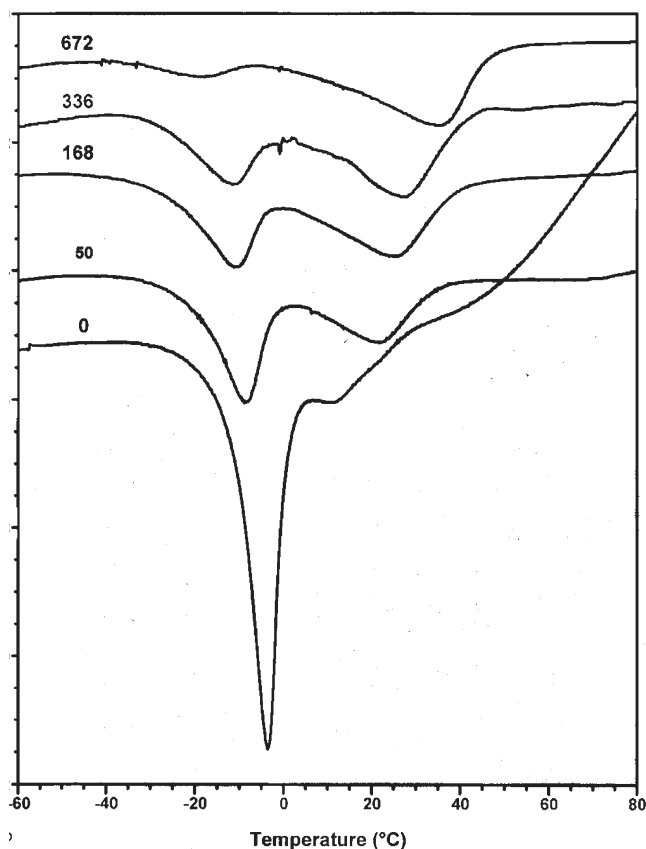


**Figure 3.** Changes in the melting endotherms of 38 wt %  $\text{Na}_2\text{K-SG}$  upon heating for various times at 40 °C. Heating times in hours are listed on the graph. The traces have been displaced vertically for clarity.

stored at ambient temperatures. These changes in melting behavior are greatly accelerated by an increase in temperature. Figure 3 shows the changes that occurred with time over a three week period for five separate samples of  $\text{Na}_2\text{K-SG-0}$  held at 40 °C in sealed tubes. The gradual decrease in the total enthalpy of melting from 24.9 to 11.7 J/g is accompanied by progressive changes in the total exothermic enthalpy of reaction from  $-56$  to  $-45$  kJ/mol M.

The shifts in the melting profiles to higher temperatures shown in Figure 3 suggest enrichment of the sodium content of the encapsulated alloy by preferential potassium dissolution in (and/or reaction with) the silica. The changes with time at 40 °C are consistent with the expected patterns that would result from removal of  $\text{K}^0$  from the encapsulated  $\text{Na}_2\text{K}$  alloy. The initial melting at  $-5$  °C is due to peritectic melting of the  $\text{Na}_2\text{K}$  compound, reduced from its bulk value of  $+6.9$  °C because of the small particle size, and broadened because of a distribution of particle sizes. As the sodium concentration in the remaining encapsulated metal increases, the peritectic melting remains, but decreases in magnitude, while the melting profile of the remaining alloy shifts to higher temperatures. The melting profile of a sample of  $\text{Na}_3\text{K}$  (which, according to the phase diagram is a mixture of the compound  $\text{Na}_2\text{K}$  and a sodium-rich phase) is similar to that of the 50 h sample shown in Figure 3, in complete agreement with this assignment.<sup>23</sup> Na NMR spectra showed that these changes in melting behavior are not accompanied by ionization of sodium, since no build-up of the  $\text{Na}^+$  NMR peak was observed (unless the samples were heated above 100 °C).

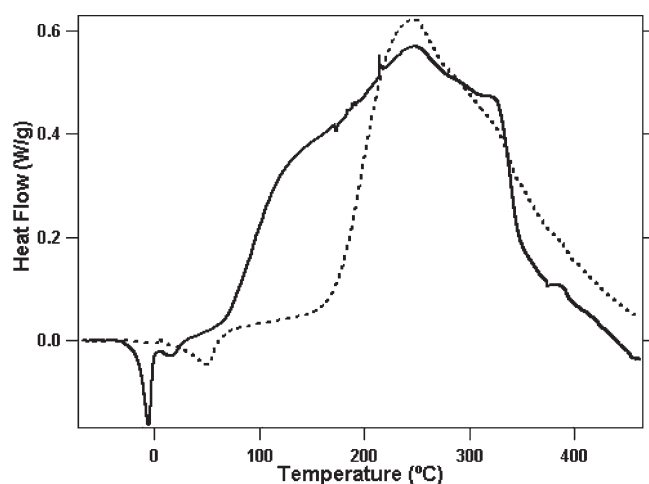


**Figure 4.** DSC traces for the conversion of 40 wt %  $\text{Na}_2\text{K-SG}$  from Stage 0 (solid) to a sample that had been heated overnight at 120 °C (dashes).

It is likely that  $\text{K}^0$  dissolves in silica and reacts much more readily than  $\text{Na}^0$ , but the formation of  $\text{K}^+$  and disappearance of  $\text{K}^0$  cannot be tested directly by  $^{39}\text{K}$  NMR because the extreme breadth of the spectrum makes it impossible to differentiate  $\text{K}^0$  from  $\text{K}^+$ . To get more information about preferential ionization, a liquid alloy of composition  $\text{Na}_2\text{KCs}$  was used to prepare a Stage 0 sample (melting endotherms at  $-35$  and  $-4$  °C). Although the  $^{133}\text{Cs}$  NMR spectrum of the sample had a poor signal-to-noise ratio, both  $\text{Cs}^0$  and  $\text{Cs}^+$  were detected in the initial sample (Supporting Information, Figure 2S). Heat treatment at 90 °C for 2 h eliminated the  $\text{Cs}^0$  NMR peak, while  $^{23}\text{Na}$  NMR showed the absence of  $\text{Na}^+$  formation. These results indicate that Cs (and presumably K) can ionize and react with silica at lower temperatures than occurs with sodium. This view is strengthened by the complete absence of a  $^{133}\text{Cs}$  NMR peak of  $\text{Cs}^0$  and the presence of a peak due to  $\text{Cs}^+$  in a sample of  $\text{Cs-SG}$  (57 wt % Cs) prepared at 40 °C. Thus, it appears likely that the changes in the melting behavior of  $\text{Na}_2\text{K-SG}$  with time at ambient temperatures and upon mild heating result from preferential incorporation of potassium in the silica and on the surface, accompanied by its ionization. This probably reflects the lower ionization energy of potassium compared with that of sodium.

As previously described, the melting behavior of  $\text{Na}_2\text{K-SG}$  changes dramatically over a period of months at room temperature and at an accelerated rate upon mild heating (Figure 3). These changes are always accompanied by changes in  $\Delta H_{\text{exo}}$ . Three samples of 40 wt %  $\text{Na}_2\text{K-SG}$ , kept at ambient temperatures for 14–16 months yielded  $\Delta H_{\text{exo}} = -37 \pm 3$  kJ/mol M. The  $^{23}\text{Na}$  NMR spectra showed no formation of  $\text{Na}^+$ . This change in  $\Delta H_{\text{exo}}$  from  $-63$  to  $-37$  kJ/mol M is nearly as great as the change to  $-27 \pm 3$  kJ/mol M for five samples heated overnight at 120–150 °C. In fact, the DSC behavior after more than a year at room temperature is very similar to that shown in Figure 4 for a sample that was heated overnight at 120 °C. Thus, solubilization of  $\text{Na}_2\text{K-SG-0}$  and its reaction with silica is exothermic and even occurs at ambient temperatures at a very slow rate (10% change in 1–3 months and nearly complete in one year). Although not investigated as fully, the thermal behavior of  $\text{K}_2\text{Na-SG-0}$  is similar, as is that of lower concentrations of  $\text{Na}_2\text{K-SG-0}$  and of samples made by using silica gel with nominal pore diameters of 6 and 4 nm.

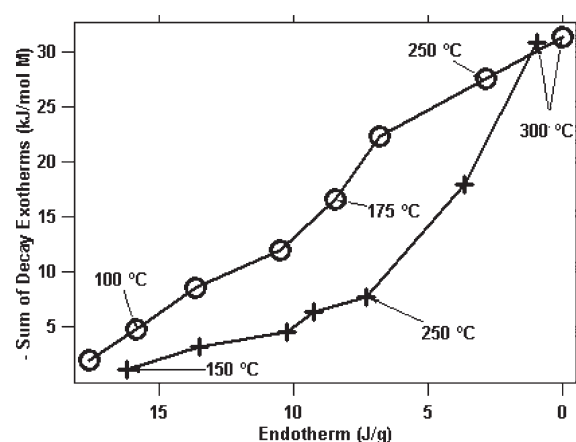


**Figure 5.** Sum of isothermal decay enthalpies at various temperatures as a function of the melting endotherm prior to each incremental temperature increase. Circles are for 38.3 wt %  $\text{Na}_2\text{K-SG}$  and plus signs are for 38.6 wt %  $\text{Na-SG}$ . Representative temperatures are indicated on the graph.

The kinetics of heat evolution of a 38.6 wt %  $\text{Na}_2\text{K-SG}$  sample was followed by DSC studies of the isothermal decay of the heat flow (power, W/g) as a function of time at eight successive temperatures between 90 and 300 °C. The sample was scanned from  $-90$  °C to the desired temperature, held for 30 min, cooled, and the procedure was repeated for the next temperature. Melting endotherms were obtained prior to each isothermal decay. At temperatures up to 90 °C there was no change in the melting endotherm and no decay of the power occurred. Thus, although both the endotherm and the exotherm decrease in days to weeks at 40 °C, the changes in 30 min are insignificant up to 90 °C. At 90 °C and above, decay of the power occurs. At 125 °C and above, each decay follows a double exponential, decaying to less than 5% of the initial rate after 30 min (Supporting Information, Figure 3S).

Because of exothermic processes that occur while heating to the isothermal temperature, the sum of all the exotherms during isothermal decays is only 69% of the total exotherm of a fresh sample obtained in a single run from 50 to 450 °C. However, the sum of the decay exotherms up to a given temperature is proportional to the change in the total fraction of metal that has melted up to that temperature, as obtained from the melting endotherms. The comparison is shown in Figure 5. An important feature of this process is that heat evolution starts immediately at each new temperature and reaches essentially zero after an hour or less. At longer times, the reactions continue at slower rates, but again, at each temperature the rate slows to near zero after overnight heating. Resumption of heat evolution then requires an increase in temperature. The general behavior described in this section has been observed for eight other samples of 40%  $\text{Na}_2\text{K-SG-0}$ , held for various times and temperatures as well as for samples with lower reducing capacities.

A similar study was made with a sample of 38.6 wt %  $\text{Na-SG}$ . Since samples had been prepared at 140–165 °C, the overall exotherm was already reduced to about  $-34$  kJ/mol Na from an expected total value of  $-50$  to  $-60$  kJ/mol Na. At each temperature between 150 and 300 °C the heat flow was followed for 2 h, during which the heat evolution decayed to zero (Supporting Information, Figure 4S). As with  $\text{Na}_2\text{K-SG}$  the biphasic decay followed a double exponential. As shown in

Figure 5, the sum of the decay exotherms was accompanied by a decrease in the melting endotherms as the metal was used up by the irreversible reaction. In another study, *separate* DSC samples of 38.6 wt % Na-SG were heated to five temperatures ( $T_{\text{iso}}$ ) between 150 and 300 °C and showed the same decay behavior (Supporting Information, Figure S5). After collection of each decay, the temperature was ramped to 450 at 20 °C/min to determine the residual values of  $\Delta H_{\text{exo}}$ . During this ramping, the power output remained at zero for about 50 °C above  $T_{\text{iso}}$  before the residual exotherm began. The magnitude of the residual exotherm following each isothermal decay decreased linearly with  $T_{\text{iso}}$  and approached zero at 350 °C.

Separate samples of Na-SG were heated for 8, 16, and 24 h at 200, 250, and 300 °C, after which they were analyzed by hydrogen evolution and DSC. The total reducing capacity for these nine samples ( $38.0 \pm 0.9\%$ ) was independent of both time and temperature. Once again, the change in the fraction of metal transferred from the pores to silica correlated with the remaining exotherm. For example, 16 h at 200 °C reduced the endotherm to 53% of its original value and the exotherm to 47%. At 250 °C the values were 21% and 19% and at 300 °C they were 2.7% and 3.4%, respectively.

These DSC studies provide convincing evidence that the exothermic reactions between sodium (and its alloys with potassium) and silica are determined by the amount of metal that has been transferred to the silica framework between exothermic decays. The limited extent of reaction at each temperature requires a “bottleneck” to the reaction processes that can only be removed by increasing the temperature. The immediate onset of exothermic reactions at each new temperature suggests that the metal had been incorporated at the previous temperature (probably as the mobile  $M^+$  and  $e^-$  species) but is unable to reduce the silica further until the temperature is increased. One possibility is that breakage of Si–O bonds and formation of Si–Si bonds is favored by small strained rings and by favorable sites for  $M^+$  localization. Further reaction may require reorganization of the silica structure. The ultimate build-up of  $\text{Na}_2\text{SiO}_3$  and Si would require significant structural changes that might be very slow and strongly temperature-dependent.

**Reaction with Alcohols.** All samples of M-SG react rapidly and completely with water to produce hydrogen. *Fresh* Stage 0 samples also do so with simple alcohols. But samples that have been heated, including all Na-SG samples, while producing hydrogen quantitatively with water, produce less with just alcohols. It is difficult to quantify this behavior because the reaction with alcohols becomes very slow at long times. Stepwise collection with an alcohol followed by water permits determination of the overall reducing capacity as well as the percent of material that is unreactive (or slow to react) with alcohols. Na-SG that has been heated overnight at 350 °C (originally called Stage II) shows no  $\text{Na}^0$  by NMR and, while it reacts quantitatively with water, it produces little or no hydrogen with completely dried alcohols. (Incidentally, the ability to react with water but not with alcohols makes Stage II Na-SG an excellent drying agent for simple alcohols). Since Stage II Na-SG contains no metal and has high concentrations of regions with Si–Si and localized  $\text{Na}^+ \text{O}^-$  bonds, this lack of reaction with alcohols suggests that Stage II regions are responsible for the decrease in the percent of heated material that reacts with water but not alcohols.

The amount of Stage II formed depends on the heat treatment used. Prolonged heating yields a saturation percentage that

depends on temperature and is reached after 10–15 h. This behavior closely resembles the isothermal decays of the exotherms described in the previous section. Representative curves are shown for  $\text{Na}_2\text{K-SG}$  and Na-SG in Figure 6.

As shown in Figure 6, the limiting fraction of Stage II regions formed in 5–20 h depends on temperature but is independent of the metal loading. The latter behavior shows that the process is not simply ionization, since the fraction of sodium that *ionizes* (determined by  $^{23}\text{Na}$  NMR) is strongly dependent on the total loading with metal.<sup>2</sup> Although the ratio  $\text{Na}^+/\text{Na}^0$  varies from sample to sample, depending on the prior heat treatment used, lower metal loadings always yield an increase in this ratio, as a higher fraction of the incorporated metal is incorporated into the silica to form  $\text{Na}^+$ . The fact that the *fraction* of Stage II formed is independent of metal loading means that depletion of the metal content by this reaction does not occur uniformly in all pores. Rather, either some pores are preferentially filled with metal while others are depleted, or partially filled pores have smaller metal clusters that are immobilized at fixed locations in the pore and do not sample all of the pore space. Evidence of sodium metal migration to enhance the amount in some pores at the expense of others was obtained by comparing the PXRD patterns of Na-SG samples at 40% and at 25% loadings. The widths of the most intense line of Na ( $2\theta = 29.4^\circ$ ,  $\text{CuK}\alpha$ ) were nearly the same for the two samples. The Scherrer relation between XRD line width and particle size<sup>31</sup> yielded average particle diameters of 10.2 and 9.5 nm for 40 and 25% loadings, respectively (Supporting Information, Figure 7S). This means that a substantial fraction of the encapsulated sodium particles have the same size, in spite of differences in loading. The growth of larger metal particles in some pores and depletion in others is energetically favored by the lower surface free energy of the larger particles. Metal migration can occur, not only intraparticle, but also interparticle, as shown by the following experiment: The  $^{23}\text{Na}$  MAS NMR spectrum of a 20% sample of  $\text{Na}_2\text{K-SG-I}$  had a  $\text{Na}^+/\text{Na}^0$  ratio that was less than that of a 10% sample. When the 20% sample was mixed with an equal amount of pure SG and heated for 12 h. at 110 °C, the sample became uniform in appearance and its  $\text{Na}^+/\text{Na}^0$  ratio was identical to that of the separately prepared 10% sample. Thus, at elevated temperatures, the metal can migrate readily from one particle to another as well as through the pores.

Although the liquid alkali metals can migrate to form filled and empty pores, this process must be preceded by some ionization throughout the sample. The ratio  $\text{Na}^+/\text{Na}^0$  increases with decreased loading for both Na-SG and  $\text{Na}_2\text{K-SG}$  samples that have been heated to 150 °C. If ionization occurred only near filled pores, we would expect the ratio to be independent of loading, as is the case for the fraction of Stage II regions formed. Thus, at least a substantial fraction of the ionization must precede the slower formation of Stage II regions, which contain Si–Si bonds produced by the formation of adjacent pairs of  $\text{Na}^+$  ions and electrons and by slow reorganization of the silica framework. Since high local concentrations of alkali metals would favor such pairwise interactions, Stage II formation would occur preferentially near metal-filled pores and would produce a fraction that was independent of loading. The overall ionization processes include not only these irreversible reactions, but presumably also the reversible formation of highly mobile  $\text{Na}^+e^-$  pairs. This point will be revisited in connection with  $^{23}\text{Na}$  NMR studies.

The formation of a limiting fraction of Stage II material at each temperature shows that the rate of conversion is not

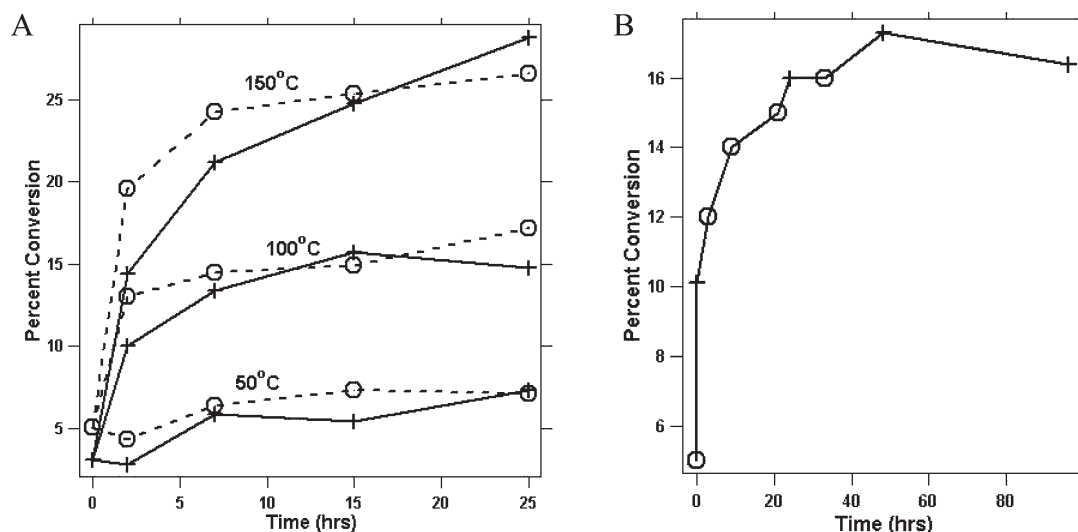


**Figure 6.** Percent formation of regions (Stage II) of M-SG that do not react with alcohols. Loadings are 20 (○) and 40 (+) wt %. (A) Na<sub>2</sub>K-SG at three temperatures. (The behavior of K<sub>2</sub>Na-SG is similar, as shown in Supporting Information, Figure 6S). (B) Na-SG at 150 °C.

characterized by a single, temperature-dependent reaction. Rather, the changes involve a series of processes that require different temperatures and that proceed to apparent completion at each temperature during a limited time period. This agrees with the earlier suggestion that the slow process required to unblock the reaction of metal with silica is reorganization of the silica structure following exothermic formation of Si–Si and irreversible breakage of Si–O bonds.

**Ionization Measurements by <sup>23</sup>Na Solid-State NMR Spectra.** Static solid-state <sup>23</sup>Na NMR spectra show widely separated peaks of Na<sup>0</sup> and Na<sup>+</sup> near 1200 and 0 ppm, respectively.<sup>32</sup> Samples of Na-SG show the presence of both Na<sup>0</sup> and Na<sup>+</sup>, and integrated intensities can be used to obtain the relative concentrations of these two species. For conducting samples, one must be concerned about attenuation of signals due to skin-depth effects. In Na-SG samples, the regions occupied by Na<sup>0</sup> and Na<sup>+</sup> are about 10 nm apart. This distance is small compared with the skin depth of metallic sodium, which is ~5 μm at this frequency (105 MHz). Thus, the power absorption should be the same in both regions.<sup>33</sup> Because of sample conductivity, considerable attenuation may occur within a sample, or even within a given particle, but the effect on Na<sup>+</sup> and Na<sup>0</sup> should be the same. To verify this assumption, numerous experiments were done with and without added sodium salts and inert diluents. Independence of delay times and phasing was also demonstrated. Because signal intensities and the resultant signal-to-noise ratios depend strongly on the overall sample conductivity and temperature, only *relative* concentrations of Na<sup>+</sup> and Na<sup>0</sup> can be obtained.

The increase in the ratio Na<sup>+</sup>/Na<sup>0</sup> of Na-SG and preheated Na<sub>2</sub>K-SG samples with a decrease in loading and/or pore size has been previously described<sup>2</sup> and was verified in this work. This ratio is a measure of both reversible and irreversible ionization and Stage II formation. It increases when the samples are heated between measurements. The time and temperature dependences are shown in Figure 7 for separate samples from a 38 wt % Na-SG preparation that had an initially low ratio of Na<sup>+</sup>/Na<sup>0</sup> (0.16 ± 0.03). At each temperature, the ratio tends to increase rapidly during the first 5–10 h of heating and then more slowly for days. The resemblance to the kinetics of heat evolution and the formation of Stage II regions is obvious.

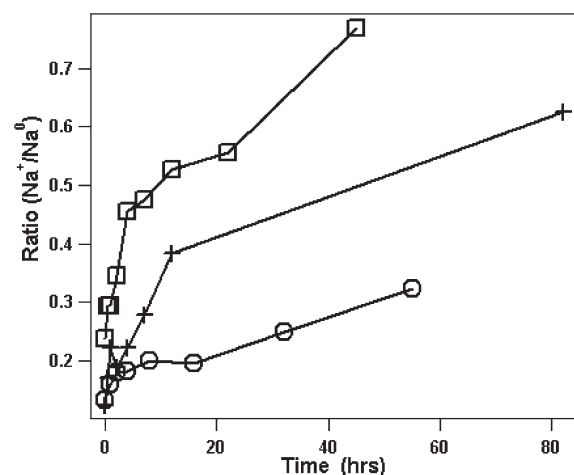


**Figure 7.** Ratio of Na<sup>+</sup>/Na<sup>0</sup> (from <sup>23</sup>Na NMR spectra at 25 °C) for three 38 wt % samples of Na-SG vs time of prior heating at three temperatures: 125 °C (○), 150 °C (+), 175 °C (□).

Both solubilization of Na in silica and the formation of Stage II regions in Na-SG produce Na<sup>+</sup> ions. By comparing the fraction of total sodium that forms Stage II with the fraction ionized, we can separate the two processes. While no systematic study on the same sample has been made, approximately half of the Na<sup>+</sup> produced by preparing Na-SG at 140–180 °C is the result of Stage II formation as determined by the fraction of material that does not react with alcohols.

**Temperature-Dependent <sup>23</sup>Na NMR Spectra.** The ratio Na<sup>+</sup>/Na<sup>0</sup> was obtained by integrating the static <sup>23</sup>Na NMR spectra taken at 25 °C. These spectra had well-separated peaks and a flat baseline between peaks. Heating or cooling the samples *in the spectrometer* produced marked changes in the spectra *that were completely reversible*. The spectra of a 40 wt % Na-SG sample at 25 and 150 °C are shown in Figure 8. Similar behavior was seen at lower loadings and for samples of Na<sub>2</sub>K-SG that had been previously heated to 150 °C. The separate peaks of Na<sup>+</sup> and Na<sup>0</sup> with zero baseline between them gradually changed with increasing temperature to yield substantial signal between the peaks. By



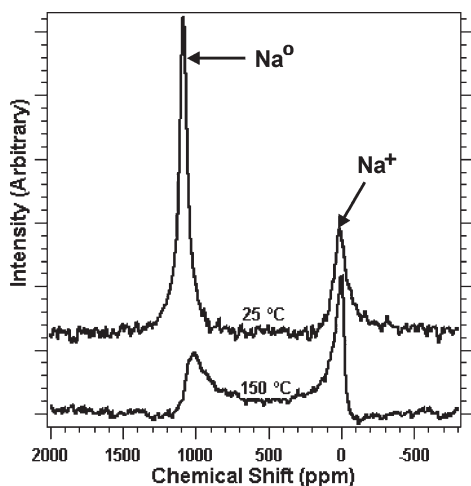


**Figure 8.** Comparison of the  $^{23}\text{Na}$  NMR spectrum of 40 wt % Na-SG at 25 °C (top) and 150 °C (bottom). The intensities were adjusted to yield the same total integral at the two temperatures.

adjusting the baseline outside of the peaks to zero we can estimate the contribution to the integrated intensity from the interpeak region. This varies from <5% of the total at 25 °C to about 30% at 150 °C.

It is known that the NMR spectra of small metal particles are broadened because of surface effects<sup>34,35</sup> and such an effect was considered to operate in NMR studies of sodium in controlled pore-size silica.<sup>36</sup> The changes with temperature observed here were not caused primarily by particle size. This was verified by measuring the temperature-dependence of the peak of  $\text{Na}^0$  in a sample of Na in alumina gel (Na-AG) with a nominal pore diameter of 9 nm. Since Na does not ionize in AG, only the peak of  $\text{Na}^0$  is present. A temperature increase to 150 °C shifted this peak slightly (from 1114 to 1130 ppm) and broadened it from 4100 to 4500 Hz, but there were no other effects of increased temperature.

While the marked spread of the  $\text{Na}^0$  peak into the intermediate region seen for Na-SG is not a direct particle-size effect, it could result from rapid diffusion of  $\text{Na}^0$  to the walls of the  $\text{Na}^0$ -filled pores. The  $\text{Na}^+$  formed at the  $\text{SiO}_2$  surface would be in contact with Na atoms that would then take on partial ionic character, as occurs with alkali metal suboxides.<sup>37</sup> Exchange with  $\text{Na}^0$  at various distances from the wall would then cause a spread of the  $\text{Na}^0$  NMR signal. The time scale for such exchange is the NMR exchange time of 1.3  $\mu\text{s}$ . The diffusion coefficient of liquid  $\text{Na}^0$  at 100 °C is  $4.2 \times 10^{-5} \text{ cm}^2 \text{ s}^{-1}$ ,<sup>38</sup> while that of solid  $\text{Na}^0$  at 25 °C is  $5.8 \times 10^{-9} \text{ cm}^2 \text{ s}^{-1}$ .<sup>39</sup> This yields root-mean-square diffusion lengths that range from 1.3 nm at 25 °C to 120 nm at 100 °C. These distances are clearly long enough to provide effective exchange between metal in the cluster and at or near the surface of the silica. Exchange with  $\text{Na}^+$  that is dissolved in the silica could also be involved if the diffusion rate of the mobile  $\text{Na}^+$  is high enough. Localized  $\text{Na}^+$  produced by irreversible reaction with silica is not involved in the exchange, so part of the  $\text{Na}^+$  signal is independent of temperature.

Three samples of 40% Na-SG at temperatures below 0 °C showed an additional narrower peak of  $\text{Na}^0$  (width = 2400 Hz) at 1130 ppm along with the broader peak (width = 9700 Hz) at 1090 ppm that is characteristic of spectra at 0 °C and above. The integrated ratio,  $\text{Na}^+/\text{Na}^0$ , dropped abruptly from 0.5 at 0 °C to 0.25 at −25 °C and remained constant down to −80 °C. The

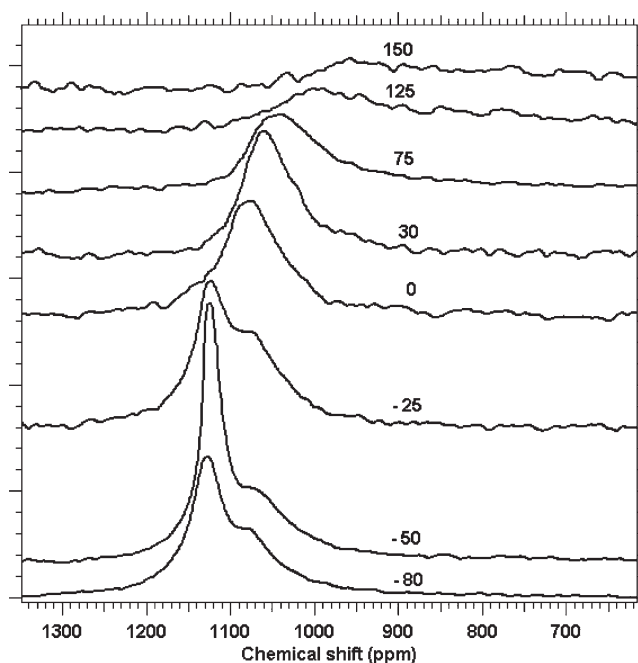


**Figure 9.** Reversible solid-state  $^{23}\text{Na}$  NMR spectra of 38.6 wt % Na-SG as a function of temperature in the  $\text{Na}^0$  region. The amplitudes were normalized to a constant value of the total integral from 1500 to −500 ppm. The spectra have been displaced vertically for clarity.

same behavior was observed with a 20% Na-SG sample. If the  $^{23}\text{Na}$  NMR spectra give valid information about the relative amounts of  $\text{Na}^0$  and  $\text{Na}^+$  present, the low temperature results indicate reversible formation of metallic sodium at −25 °C and below by conversion of mobile  $\text{Na}^+ \cdot \text{e}^-$  in the silica and on the surface to sodium metal in the pores. However, the possibility that the relative sensitivities to  $\text{Na}^0$  and  $\text{Na}^+$  may be temperature-dependent cannot be ruled out.

The marked effect of temperature on the spectrum in the chemical shift region of  $\text{Na}^0$  is shown in Figure 9. The amplitudes were normalized to a constant value of the total integral from 1500 to −500 ppm. Complete spectra are shown in Supporting Information, Figure 8S.

## SUMMARY AND CONCLUSIONS

Three types of measurement were used to characterize the nature of alkali metal–silica gel interactions:

- (1) Quantitative collection of hydrogen produced by the successive addition of a simple alcohol and water showed that the reducing capacity of the added alkali metal is retained, even when prior reaction with the silica has occurred. Reduction of the fraction of the hydrogen produced by the addition of alcohol was used as a measure of the extent of formation of Si–Si bonds and localized  $\text{M}^+-\text{O}^-$ -Si species. The concentration independence of the fraction of metal involved, together with the PXRD measurements of the sodium metal particle size, indicated that metal migration occurred to fill some pores and empty others.
- (2) DSC measurements were used to study the melting behavior of encapsulated metal particles and the kinetics and thermodynamics of exothermic reactions between the alkali metal and silica. Both the melting temperature



and the enthalpy of melting are reduced because of the small size of the metal inclusions. The shift of the melting endotherms of Na<sub>2</sub>K-SG samples with time and temperature indicated that potassium is preferentially incorporated into the silica compared with sodium.

(3) Solid-state <sup>23</sup>Na NMR studies as a function of temperature and concentration showed that the encapsulated Na<sup>0</sup> nanoparticles undergo rapid exchange with Na<sup>+</sup>, located at the surface or in the bulk of the silica framework. At temperatures below about −20 °C, there is an indication of the reversible formation of Na<sup>0</sup> by removal of dissolved and ionized sodium from the silica, although this behavior could be the result of incomplete penetration of the RF field into the particles.

These studies indicate that alkali metals can interact with nanoporous silica gel in at least three ways:

- (1) The metal can fill the empty pores to form metallic nanocrystals at low temperatures and liquid nanodroplets of alkali metals or their alloys at higher temperatures. The melting points and enthalpy of melting are reduced from those of the bulk metals because of both the small particle sizes and transfer of part of the metal to the silica. At loadings below those required to fill all pores with metal, migration occurs to fill some pores and empty others.
- (2) According to literature studies, alkali metals are reversibly soluble in thin silica films under vacuum, accompanied by ionization and electron transfer to the silica.<sup>25–27</sup> The cation and the released electron, are mobile, with a diffusion rate estimated to be on the picosecond time scale.<sup>27</sup> These studies presumed rapid and reversible breakage of Si–O bonds to form Na<sup>+</sup>–O<sup>−</sup>–Si units when Na dissolves in silica,<sup>26</sup> but the equal coordination of Na<sup>+</sup> to three oxygens requires rapid exchange of the negative charge around the ion. An attractive alternative is electron transfer from the metal atom to delocalized states of the silica to form an “inorganic electride”<sup>18</sup> such that the hopping of M<sup>+</sup> from site-to-site is fast and is accompanied by electron mobility. This would not require Si–O bond breakage, but whether it would give the observed oxygen-1s XPS behavior similar to that of unbridged oxygen anions<sup>26</sup> is unknown. The two alternatives are shown schematically in Figure 1. Such solubilization may also occur in alkali metal–silica gel materials, but we have no way to distinguish formation of localized Na<sup>+</sup>–O<sup>−</sup>–Si sites from mobile Na<sup>+</sup>·e<sup>−</sup> species.
- (3) Irreversible reduction of silica leads to the formation of Si–Si bonds and localized Na<sup>+</sup>–O<sup>−</sup>–Si species. The localization reactions may be responsible for most of the exothermic heat of reaction. They tend to reach a limit in a few hours at each temperature such that further reaction requires either much longer times or an increase in temperature. Regions of such irreversible reactions that form Si–Si bonds occur preferentially near the metal-filled pores and are characterized by their inability to produce hydrogen by reduction of simple alcohols.

## ■ ASSOCIATED CONTENT

**S Supporting Information.** Further details are given in eight figures, Figures 1S–8S. This material is available free of charge via the Internet at <http://pubs.acs.org>.

## ■ AUTHOR INFORMATION

### Corresponding Author

\*E-mail: [dye@msu.edu](mailto:dye@msu.edu) (J.L.D.), [michael@signachem.com](mailto:michael@signachem.com) (M.L.).

## ■ ACKNOWLEDGMENT

We are grateful to the Camille and Henry Dreyfus Foundation Senior Scientist Mentor Program for support of the seven undergraduate coauthors. SiGNa Chemistry Inc. provided scientific discussion and financial support. We acknowledge Vernon Swope for measuring Raman spectra, Kermit Johnson and Daniel Holmes for help with NMR studies, Rui Huang for powder X-ray measurements, and Michael Beach and Andrea Alexander for various analyses.

## ■ REFERENCES

- (1) Dye, J. L.; Cram, K. D.; Urbin, S. A.; Redko, M. Y.; E., J. J.; Lefenfeld, M. *J. Am. Chem. Soc.* **2005**, *127*, 9338–9339.
- (2) Shatnawi, M.; Paglia, G.; Dye, J. L.; Cram, K. D.; Lefenfeld, M.; Billinge, S. J. L. *J. Am. Chem. Soc.* **2007**, *129*, 1386–1392.
- (3) Burns, J. A. *Glass Technol.* **1963**, *6*, 17–21.
- (4) Lau, J.; McMillan, P. W. *J. Mater. Sci.* **1982**, *17*, 2715–2726.
- (5) Lau, J.; McMillan, P. W. *J. Mater. Sci.* **1984**, *19*, 881–889.
- (6) Fatt, I.; Tashima, M. *Alkali metal Dispersions*; D. Van Nostrand: Princeton, N.J., 1961.
- (7) Contento, M.; Savoie, D.; Trombini, C.; Umani-Ronchi, A. *Synthesis* **1979**, *1*, 30–32.
- (8) Levy, J.; Tamarkin, D.; Selig, H.; Rabinovitz, M. *Angew. Chem., Int. Ed. Engl.* **1981**, *20*, 1033.
- (9) Singh, S.; Dev, S. *Tetrahedron* **1993**, *49*, 10959–10964.
- (10) Furstner, A.; Seidel, G. *Synthesis* **1995**, 63–68.
- (11) Makoza, M.; Nieczypor, P.; Grela, K. *Tetrahedron* **1998**, *54*, 10827–10836.
- (12) Rabo, J. A.; Angell, P. H.; Kasai, P. H.; Schomaker, V. *Faraday Discuss.* **1966**, *41*, 328–349.
- (13) Edwards, P. P.; Anderson, P. A.; Thomas, J. M. *Acc. Chem. Res.* **1996**, *29*, 23–29.
- (14) Srdanov, V. I.; Haug, K.; Metiu, H.; Stucky, G. D. *J. Phys. Chem.* **1992**, *96*, 9039–9043.
- (15) Li, Z.; Yang, J.; Hou, J. G.; Zhu, Q. *J. Am. Chem. Soc.* **2003**, *125*, 6050–6051.
- (16) Ichimura, A. S.; Dye, J. L.; Camblor, M. A.; Villaescusa, L. A. *J. Am. Chem. Soc.* **2002**, *124*, 1170–1171.
- (17) Petkov, V.; Billinge, S. I.; Ichimura, A. S.; Dye, J. L. *Phys. Rev. Lett.* **2002**, *89*, 075502.
- (18) Wernette, D. P.; Ichimura, A. S.; Urbin, S. A.; Dye, J. L. *Chem. Mater.* **2003**, *15*, 1441–1448.
- (19) Nandi, P.; Redko, M. Y.; Petersen, K.; Dye, J. L.; Lefenfeld, M.; Vogt, P. F.; Jackson, J. E. *Org. Lett.* **2008**, *10*, 5141–5144.
- (20) Nandi, P.; Dye, J. L.; Bentley, P.; Jackson, J. E. *Org. Lett.* **2009**, *11*, 1689–1692.
- (21) Nandi, P.; Dye, J. L.; Jackson, J. E. *J. Org. Chem.* **2009**, *74*, 5790–5792.
- (22) Nandi, P.; Dye, J. L.; Jackson, J. E. *Tetrahedron Lett.* **2009**, *50*, 3864–3866.
- (23) Bodnar, B. S.; Vogt, P. F. *J. Org. Chem.* **2009**, *74*, 2598–2600.
- (24) [www.signachem.com](http://www.signachem.com), U. S. p. N., 211,539;7, 560,606.
- (25) Lagarde, P.; Flank, A.-M.; Mazzara, C.; Jupille, J. *Surf. Sci.* **2001**, *482–485*, 376–380.
- (26) Mazzara, C. J., J.; Flank, A.-M.; Lagarde, P. *J. Phys. Chem. B* **2000**, *104*, 3438–3445.
- (27) Jupille, J.; Flank, A.-M.; Lagarde, P. *J. Am. Ceram. Soc.* **2002**, *85*, 1041–1046.
- (28) Rarivomanantsaa, M. J., P.; Jullien, R. *J. Chem. Phys.* **2004**, *120*, 4915–4920.

- (29) Unruh, K. M.; Huber, T. E.; Huber, C. A. *Phys. Rev. B.* **1993**, 48, 9021–9027.
- (30) Buffat, P.; Borel, J.-P. *Phys. Rev. A* **1976**, 13, 2287–2298.
- (31) Patterson, A. L. *Phys. Rev.* **1939**, 56, 978–982.
- (32) Knight, W. D. *Phys. Rev.* **1944**, 76, 1259–1260.
- (33) Bloembergen, N. *J. Appl. Phys.* **1952**, 23, 1383–1389.
- (34) Charles, R. J.; Harrison, W. A. *Phys. Rev. Lett.* **1963**, 11, 75–77.
- (35) Bercier, J. J.; Jirousek, M.; Graetzel, M.; van der Klink, J. J. *J. Phys.: Condens. Matter* **1993**, 5, L571–L576.
- (36) Terskikh, V. V.; Moudrakovski, I. L.; Ratcliffe, C. I.; Ripmeester, J. A.; Reinhold, C. J.; Anderson, P. A.; Edwards, P. P. In *Magnetic Resonance in Colloid and Interface Science*; Lapina, J. F. a. O., Ed.; Kluwer Academic Publishers: Amsterdam, 2002; pp 469–474.
- (37) Simon, A. In *Molecular Clusters of the Main Group Elements*; Driess, M., Noth, H., Eds.; Wiley-VCH: Weinheim, Germany, 2004; pp 246–266.
- (38) Meyer, R. E.; Nachtrieb, N. H. *J. Chem. Phys.* **1955**, 23, 1851–1854.
- (39) Mundy, J. N. *Phys. Rev. B.* **1971**, 3, 2431–2445.